Flood-Induced Recharge of Matrix Water in a Vertic Forest Soil

Savannah R. Morales[1,2], Mary Grace T. Lemon[1,3], Ryan D. Stewart[4], and Richard F. Keim[1]

[1]School of Renewable Natural Resources, Louisiana State University, Baton Rouge, LA, USA. [2]Providence Engineering and Environmental Group LLC, Baton Rouge, LA, USA. [3]US Fish and Wildlife Service, Minneapolis, MN, USA. [4]School of Plant and Environmental Sciences, Virginia Tech University, Blacksburg, VA, USA

Corresponding author: Richard Keim (rkeim@lsu.edu)

Key Points:

- Infiltration of floodwater via macropores ceased with swelling, but isotopic composition was heterogeneous even after 31 d of inundation
- Slow diffusion dominates isotopic evolution of soil matrix water in Vertisols as porosity decreases
- The importance of flooding as a source of matrix recharge in vertic floodplain soils may depend more on flood frequency than duration

Abstract

Vertisols shrink and swell with changes in soil moisture, influencing hydraulic properties. Vertisols are often in floodplains, yet the importance of flooding as a source of soil moisture remains poorly understood. We used blue dye and deuterated water as tracers to determine the role of the macropore network in matrix recharge under artificial flood durations of 3 and 31 d in large soil monoliths extracted from a forested soil. Gravimetric soil moisture content increased by 47% in the first three days, then increased only 3.5% from day 3 to 31. Post-flood moisture content was greatest in the organic-rich, top 10 cm and was lower at 10 to 75 cm where organic matter was less. Deuterium concentration revealed that soil moisture in the top 10 cm was quickly dominated by artificial flood water, but at depth remained <80% floodwater even after 31 d. Pervasive dye staining of ped surfaces in the top 4 cm indicated connectivity to flood waters but staining at depth was less and highly variable. The isotopic composition of soil water at depth continued to shift toward flood water despite no differences in dye staining between days 3 and 31. Results indicate flooding initially but incompletely recharges matrix water via macropores and suggest the importance of flooding as a source of matrix recharge in vertic floodplain soils may depend more on flood frequency than duration. Isotopic composition of matrix water in vertic soils depends on both advective and diffusional processes, with diffusion becoming more dominant as porosity decreases.

Plain Language Summary

Shrink-swell clay soils are common in floodplains but their behavior during flooding, particularly how much flood water they take up, is not well understood. We flooded large blocks of shrink-swell soil with artificial floodwater spiked with dye and chemically-labeled water, and found that water moved rapidly into soils via cracks and large soil pores, but swelling closed those pathways and prevented floodwater from spreading throughout the soil blocks. Only near the surface, where there is more organic matter, did floodwaters completely dominate soil moisture after flooding. Results indicate that flow into cracks in shrink-swell soil is important early in a flood, but not enough water flows this way to allow floodwater to reach throughout the soil before the clays swell and close those pathways. Because the amount of water that the soil can take up is limited in each event, the importance of flooding for soil moisture in shrink-swell clay soils in floodplains depends on how often flooding occurs rather than how long it persists.

1 Introduction

Fine-grained Vertisols are globally distributed and occupy approximately 2.4% of the earth's non-ice-covered surface (USDA-NRCS, 1999). Vertisols and related vertic intergrades are distinct because the smectitic clays that compose them impart shrink-swell properties that are a function of soil moisture (Groenevelt & Bolt, 1972; Das Gupta et al., 2006). At low moisture content the soil matrix shrinks, resulting in a heterogeneous network of cracks that readily transmit water in macropores. At high moisture content the matrix swells, partially closing the crack network and greatly reducing permeability. Thus, water flow paths are dynamic in both space and time (Stewart et al., 2015).

In Vertisols, the cracks and slickensides that form the boundaries of soil peds are macropores that conduct the majority of water, though not all macropores are connected and carry flow (Bouma et al., 1977; Yasuda et al., 2001). Vertic soils can become episaturated in some cases, meaning saturation of a surface- or near-surface layer and unsaturated below (Kishné et al., 2010). They can also develop local and discontinuous zones of saturation, affiliated with macropores, that do not necessarily connect to each other (Bouma et al., 1980; Armstrong 1983; Booltink & Bouma 1991). Upon wetting, cracks can close within hours (Favre et al., 1997) and shift hydraulic conductivity (Ksat) from predominantly macropores flow to diffusional matrix flux (Bronswijk et al., 1995; Stewart et al., 2016b).

Despite numerous studies and models devoted to quantifying matrix and macropore flow (e.g., Flury et al., 1994; Hardie et al., 2013; Stewart et al., 2016), many hydrological processes in vertic clay soils remain poorly understood. For example, research to quantify vertic soil matrix recharge by precipitation has been extensive (e.g., Hoogmoed & Bouma, 1980; Römkens & Prasad, 2006), but the role of flood duration and ponding in soil moisture recharge has not been extensively investigated. Many vertic soils occur in current or former floodplains and lake bottoms, where landforms and topographic position are often conducive to flooding or ponding. Flooding plays a crucial role in influencing floodplain ecosystems through flood stress on plants, but it may also recharge soil moisture later used by plants (e.g., Lamontagne et al., 2005; Allen et al., 2016). Most field investigations of Vertisol hydrology under flooded conditions have focused on flux through macropores, focusing on the crack network (e.g., Bouma & Wösten, 1984) or on

how the crack network is modified by soil swelling upon ponding (e.g., Favre et al., 1997). There are reasons to expect the consequences of flooding for matrix moisture recharge may be larger than rainfall because flooding provides near-infinite water supply at high pressure potential, which can drive rapid infiltration through crack networks perhaps more rapidly than they can close. Alternatively, flooding may only induce limited recharge if matrix swelling closes cracks after infiltration of relatively small volumes of water. In the latter case, pre-event soil moisture may still dominate even after flooding.

The enigmatic and poorly understood mechanisms controlling recharge of vertic soils have important implications for ecosystems. Soil moisture recharge, retention, and depletion are some of the most important processes governing ecosystem function. Most precipitation over land returns to the atmosphere as transpiration (Jasechko et al., 2013, Good et al., 2015), with the soil matrix acting as the primary temporary store for this water. Water residence times in soil vary over many orders of magnitude, and transpiration tends to draw on older, rather than the most recently infiltrated, water (Berghuijs & Allen, 2019). This process creates a temporal decoupling between matrix recharge and uptake by plants, which can obscure sources of this important water store. Isotopic tracers have indicated separation between transpired water and younger water draining from soils in some cases (e.g., Brooks et al., 2010; Goldsmith et al., 2012; Allen et al., 2019), but mixing and isotopic exchange can complicate interpretations (e.g., Oshun et al., 2016; Bowling et al., 2017; Vargas et al., 2017). Thus, considerable uncertainty remains about the hydrological sources of water available to plants in all soils, let alone in hydrologically complex, vertic soils.

The goal of this research was to empirically quantify flood recharge of soil matrix water in a forested Vertisol, focusing on the role the macropore network plays in delivering water to the matrix. To do this, we conducted an artificial flooding experiment on soil monoliths transported intact to the laboratory. We used two tracers in our floodwater: (1) a sorbing, dye tracer to estimate connectedness of individual soil peds to the macropore network at multiple depths in the soil profile; and (2) a conservative tracer (deuterium) to estimate mass flux into peds. We hypothesized that soil peds most connected to the macropore network, as evidenced by dye-staining, would also attain the greatest isotopic enrichment.

2 Materials and Methods

2.1 Experiment Overview

We imposed artificial flooding on soil monoliths excavated intact from a forested Vertisol. The treatment monoliths were submerged in dyed and isotopically spiked water in short (3–4 days) versus long (31–32 days) artificial floods. After treatment, the monoliths were deconstructed to extract individual peds that were then analyzed for dye coverage, stable isotopic composition of soil water, moisture content, and organic matter content. Control monoliths were also deconstructed and analyzed for the same variables to quantify conditions prior to the artificial floods.

2.2 Field Sampling

The study site is in the floodplain of the Mississippi River near St. Gabriel, Louisiana (30°16'54" N, 91°05'21" W). Levees have prevented overbank flooding from the Mississippi River for more than 200 yr but the site is frequently inundated by ponded precipitation from late winter through spring. The mean annual precipitation is 158 cm and the mean annual temperature is 20°C. The site is occupied by a mixed-species floodplain forest dominated by sugarberry (*Celtis laevigata*), American elm (*Ulmus americana*), and green ash (*Fraxinus pennsylvanica*), with the last logging more than 60 yr in the past.

The soil met the criteria for a Sharkey clay, classified as a very-fine, smectitic, thermic Chromic Epiaquert in the Soil Taxonomy system, and as a Pellic Vertisol (Gleyic, Hypereutric, Ochric, Stagnic) in the World Reference Base system. At the surface is an organic-rich horizon where there is little structure except for common, small, granular, “buckshot” (Broadfoot, 1962) aggregates. Below, the soil is composed of weak, medium (<30 mm) peds that are subangular and blocky or wedge-shaped with slickenside boundaries typical of Vertisols—the latter increasing below 20 cm. At the time of sampling in September 2018 (Figure 1), the soil was relatively dry and visibly cracked on the surface. Many fine- to medium-sized roots were present, especially in the top 40 cm; the largest root in any of the monoliths was ~1 cm diameter. Ped boundaries tended to be formed on sides of medium-sized roots, and there were no peds formed completely around medium roots. Fine roots (≤ 2 mm) were found within peds.

The monoliths were cylinders pairs, each 46 cm diameter and 35 cm tall, excavated from depths of 0–35 cm and 40–75 cm. Care was taken to ensure monoliths remained intact with as little disturbance as possible by gently excavating the surrounding soil, avoiding smearing (Figure 1b). The monoliths were transferred to metal containers (each was one half of a 114 L steel drum, open on the top and pre-drilled with 1 cm holes spaced 5–8 cm apart on the bottom and sides to allow relatively free movement of water) and temporarily wrapped in plastic and cushioned to prevent evaporation and stabilize the monoliths for transportation to the laboratory. Monoliths were transferred into the metal containers using thin, open-weave, cotton cloth, which remained in place for the duration of the experiment to improve soil stability during handling.

The intent of the perforated containers was to simulate conditions of flooding a forest soil that contains root channels and other biogenic macropores. By necessity, the monoliths were excavated to avoid large roots, and did not include all heterogeneities present at the field scale. The experimental design approximates conditions near macropores, under the assumption that the macropore network allows rapid flux of floodwater to depth and lateral gradients away from macropores are as relevant for soil moisture as are vertical gradients (Greve et al. 2010). Two smaller control monoliths, 26 cm diameter, were also excavated from 0–35 cm and 40–75 cm depths and wrapped in plastic prior to transport to the laboratory. These two monoliths were used to assess pre-flood soil properties, separately from the two artificially flooded pairs of monoliths.

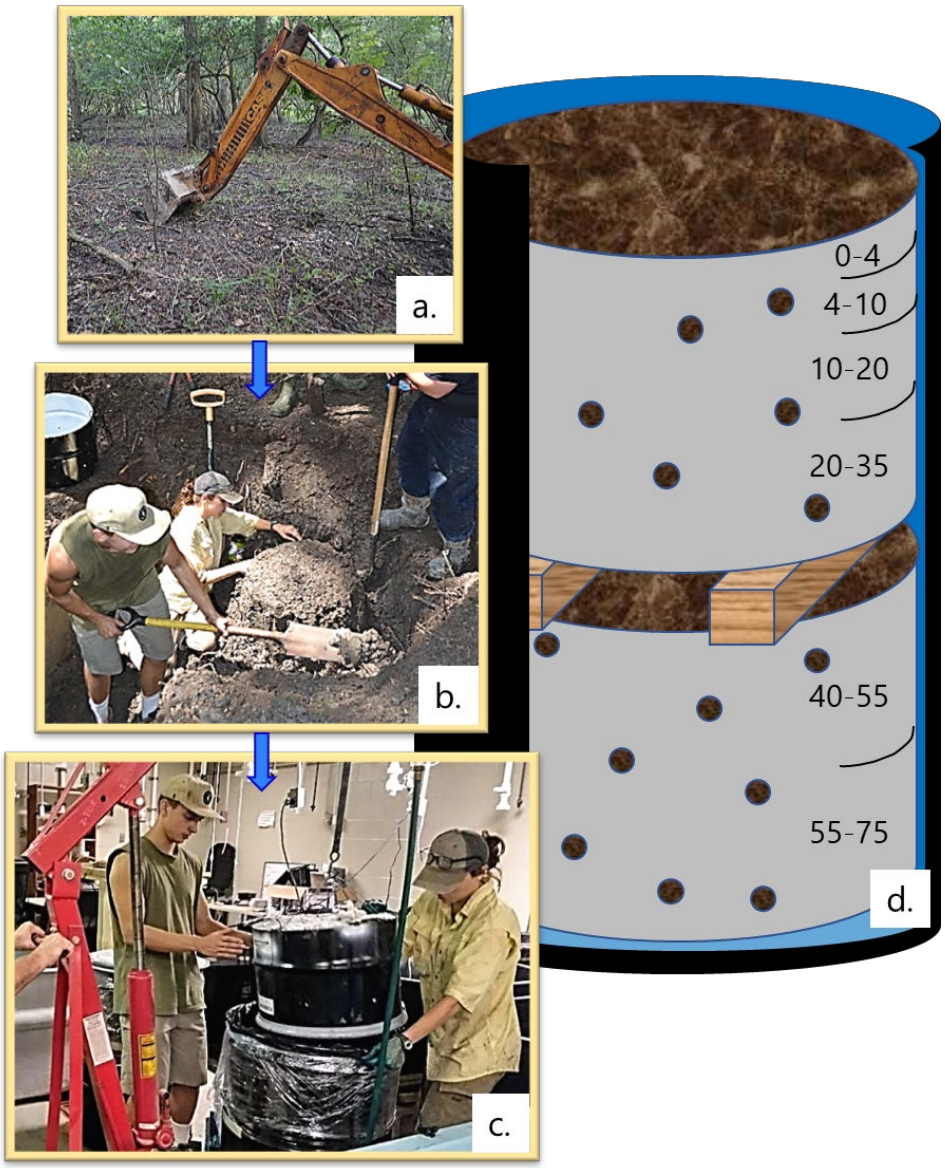

Figure 1. Sampling and experimental setup: (**a**) initial excavation of a trench; (**b**) manual excavation of a monolith adjacent to the trench; (**c**) lowering a monolith into a tank of artificial floodwater; (**d**) schematic of the paired moniliths in perforated containers submerged in artificial floodwater, omitting the thin, open-weave, cotton cloth wrappers around each ped.

2.3 Artificial Flooding with Tracers

In the laboratory, the soil monoliths were placed inside 208 L steel drums, with those excavated from 40–75 cm depth placed on the bottom of the drums and the shallower monoliths placed on top of them. Two 5 cm tall wooden spacers were used to separate upper and lower monoliths

(Figure 1d). This arrangement allowed for relatively high exposure to floodwaters of the external portions of all monoliths, simulating networks of large macropores encompassing each monolith. Also, the perforated metal containers used to hold the monoliths constrained lateral expansion of the monoliths but allowed for vertical swelling at the surface of each monolith.

To determine macropore-matrix connectivity and water exchange during flooding, two tracers were added to the flood treatment tanks prior to submerging the monoliths. Each tank contained 1 g L^{-1} blue dye (variously known as FD&C Blue #1, C.I. 42090, Brilliant Blue FCF, and C.I. Food Blue 2) as a semi-quantitative, sorbing tracer of advective flux (Flury & Flühler, 1995; Ketelsen & Mayer-Windel, 1999; Öhrström et al., 2004). This dye is commonly used in soil water flux tracing (Flury et al., 1994; Weiler & Flühler, 2004; Hardie et al., 2013), although we used a lower concentration due to a smaller ratio of soil volume to water volume as compared to most field experiments. Each tank was also spiked with deuterated water (98 atomic %) as a non-sorbing, conservative tracer of water movement. The initial soil water isotopic composition was δD = +3‰ at the surface, -5‰ at 25 cm depth, and -15‰ at 65 cm depth. The added floodwaters isotopic composition was δD = +68‰ (tank with short-duration flooding) and δD = +70‰ (tank with long-duration flooding). All isotopic values are reported per mil (‰) as $\delta D = (R_{sample}/R_{standard} - 1)*1000$, where R = D/H in either the sample or Vienna Standard Mean Ocean Water (VSMOW).

On the same day as excavation, the monoliths were fully submerged in the spiked floodwater, simulating a flood of ~3 cm depth above the soil surface. The large drums were sealed to prevent evaporation and isotopic fractionation. After 3 days, one shallow monolith was removed from the floodwaters, and the paired, deeper monolith was removed one day later. Monoliths for the long-duration artificial flooding treatment were removed after 31 (upper monolith) and 32 (lower monolith) days. These flood durations are representative of typical flood events in floodplains of the southeastern U.S. The lower monoliths were removed one day after the upper monoliths to avoid isotopic fractionation while waiting for deconstruction of the upper monolith (sec. 2.3).

200 ### 2.4 Soil and Water Sampling

201 Upon removal from the drums, monoliths were each allowed to freely drain for 20 minutes to
202 remove gravitational water from macropores. Next, the thin (<1 cm) layer of litter at the surface
203 and exterior soil, ~2 cm on top, bottom, and sides was discarded as disturbed (except no soil was
204 discarded from the top of the surface monolith). The remaining material was manually
205 deconstructed by separating peds along natural lines of fracture to obtain treatment peds for
206 analysis of dye coverage and δD (Figure 2). Ped excavation was performed using a knife tip and
207 gently plucking out naturally structured peds. Peds that broke or appeared disturbed were
208 discarded. Care was taken not to smear the soil or otherwise alter the ped surface. Also, care was
209 taken to reduce evaporative fractionation of soil water by keeping the samples covered as much
210 as possible and completing manual deconstruction within 11 hr.
211
212 Peds were obtained from depth classes 0–4, 4–10, 10–20, 20–35, 40–55, and 55–75 cm. Soil
213 properties in the upper 20 cm varied in structure more than below 20 cm, and smaller depth
214 classes were designated there to account for this variability. Obtaining structured peds was also
215 more difficult in the upper 20 cm due to high organic matter, and soil aggregates were smaller
216 and more granular than the soil from deeper depths. Control peds were processed using the same
217 methods as flood peds except depth classes were 0–4 cm, 4–35 cm, and 40–75 cm. Note that the
218 methodology required peds of at least 3 g wet mass to provide sufficient water for isotopic
219 analysis, so samples that did not meet this criterion were discarded. A total of 392 usable peds
220 were collected, including 53 control peds, 162 short flood duration peds, and 177 long flood
221 duration peds. Sampled ped size varied little by depth.
222

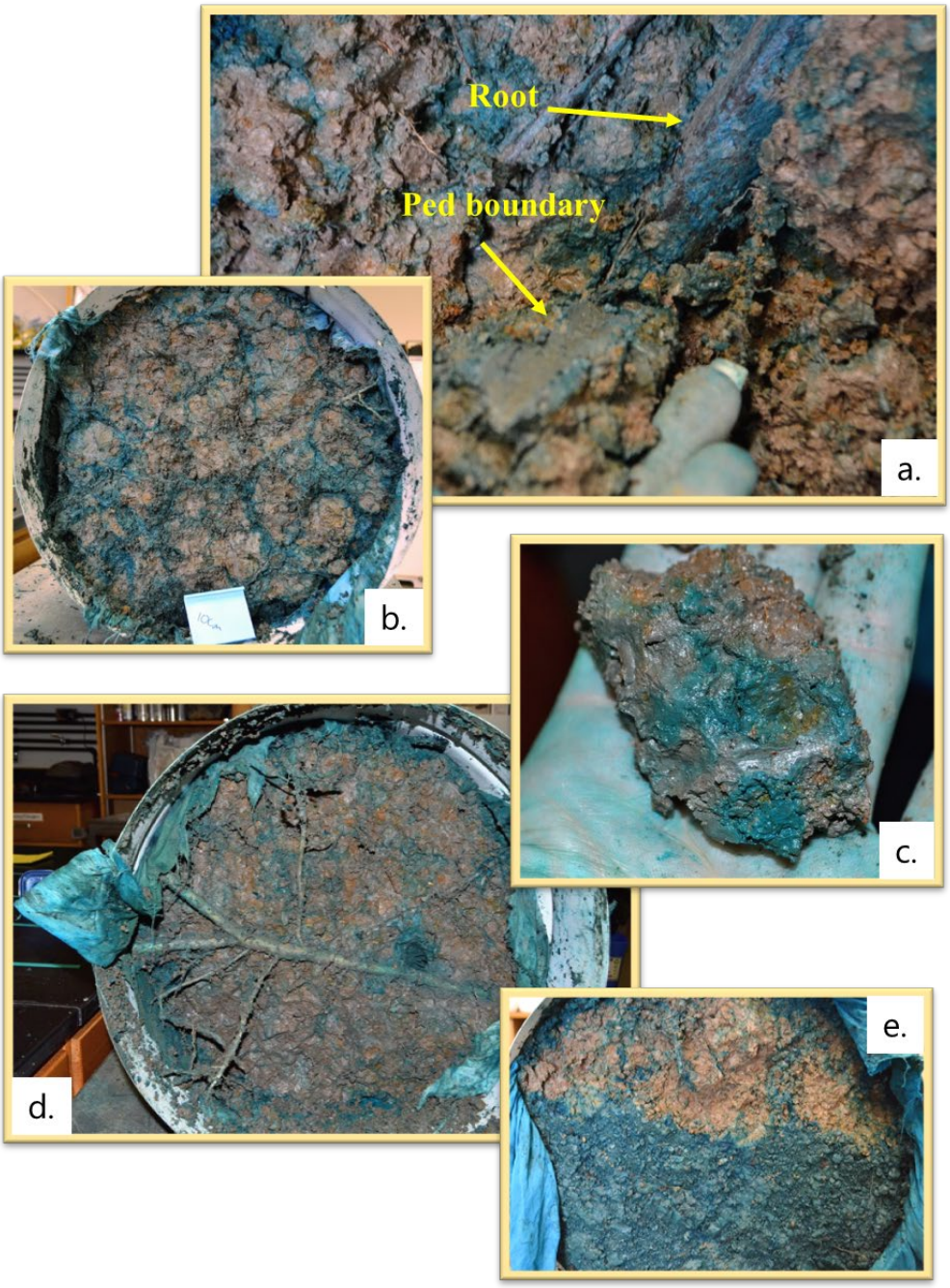

223

224 **Figure 2**. Dye staining revealed during deconstruction of monoliths: (**a**) stained root and adjacent ped
225 boundary illustrating preferential flow along roots; (**b**) top-down view of a monolith after the removal of
226 the surface 10 cm, illustrating preferential infiltration via a small proportion of the cross-section; (**c**)
227 manually removed ped illustrating partial dominance of slickensides and incomplete staining of ped
228 surface; (**d**) top-down view of a monolith after the removal of the surface 20 cm, illustrating a zone of
229 strong staining by preferential flow (center right) and common, but not ubiquitous, staining of the

rhizosphere; (**e**) top-down view of a monolith after partial removal of the top 4 cm, illustrating the rapid transition to highly preferential flow (top half of the image).

Once a ped was separated from a monolith, it was visually inspected for coverage of blue dye and assigned to a class of 0–20, 21–40, 41–60, 61–80, or 81–100 percent dye coverage. Classification was done by the same person throughout the experiment to ensure consistency. We used this simplified classification scheme because subsequent analysis for isotopic composition required us to work quickly to avoid fractionation during sample processing.

After dye coverage estimation, each ped was immediately placed into a sample bag for analysis of isotopic composition by equilibration with vapor (Wassenaar et al., 2008). Each bag was a 10 L, side-gusseted metalized plastic coffee bag (PBFY Flexible Packaging; Gralher et al., 2018) that was inflated with ambient air, heat sealed, and incubated for isotopic equilibration between soil water and vapor for 2–3 days before analysis of the vapor by laser ablation spectroscopy (Los Gatos Research IWA–45–EP). Equilibration was in the same room as the isotope analyzer and recording thermometers (Onset HOBO) recorded the room temperature every 15 or 30 minutes during this period to ensure consistency of temperature and thus equilibration between water and vapor. Bags containing liquid water standards for calibration were made on the same day as monolith deconstruction and equilibrated and analyzed following the same method as the ped bags. Precision of the δD in this experiment was ±1‰, estimated as the variance in values obtained by analyzing bags containing standards analyzed as samples.

To infer soil water δD from vapor δD, we used free-liquid α (i.e., the temperature-dependent equilibration factor between vapor and liquid in a closed system), using recorded laboratory temperature and constants reported by Majoube (1971). We also performed an empirical control by analyzing vapor in the bags containing liquid water standards of known isotopic composition. We did not correct for fractionation known to occur by water sorbing onto surfaces (Lin and Horita, 2016; Lin et al., 2018; Oerter et al., 2014), by hydration spheres formed around solutes (Oerter et al., 2014), or by wetting of organic matter (Gaj et al., 2019). Comparing maximum measured soil-water δD (+79‰) to liquid δD in the submersion tanks after the experiment (+68‰ or +70‰), we estimated that ignoring effects of soil-surface and solute chemistry on our

measurement may have caused error up to maximum 9‰, which is an order of magnitude smaller than the difference between pre-experiment water and the spiked floodwater (65–85‰). Errors likely vary throughout the dataset because of varying mineralogy, solutes, and organic matter, so we report raw measurements instead of attempting corrections.

It is possible that isotopic equilibration between water in peds and in the vapor in the bags preferentially involved water near the surfaces of peds. If that were the case, the isotopic composition of the vapor may not have reflected the isotopic composition of the liquid in the entire ped. To assess this possibility, a separate experiment was conducted to test (1) whether the peds were fully equilibrating in the vapor bag during isotopic analysis and (2) whether any disequilibrium was related to ped size. Additional control and artificially flooded peds were processed using the same vapor bag equilibration methods as the main experiment, but with the exception that some peds (16 control and 22 treatment peds from soil soaked 24 h) were crumbled before being placed inside of the vapor bag and some (15 control and 22 treatment peds from soil soaked 24 h) were left whole and placed inside the vapor bags as for the main experiment. In the control group, there was no significant difference between the crumbled and whole peds (t-test $p = 0.8$, crumbled $\delta D = -16 \pm 1$‰ s.d., whole $\delta D = -16 \pm 1$‰). In the treatment group, there was high variance but no significant difference between the crumbled and whole peds (t-test $p = 0.3$, crumbled $\delta D = +6 \pm 20$‰, whole $\delta D = 0 \pm 18$‰). The high variance in the treatment batch likely reflected the varying positions of the peds within the soaked soil monolith. Given these results, we concluded that sampling vapor equilibrated over whole, non-crumbled peds did not predictably bias the isotopic results, and that any plausible methodological effects were small relative to the difference between spiked, artificial floodwater and pre-treatment water.

To infer the contribution of floodwater to ped moisture, we compared moisture content and δD in control and post-flood peds. For isotopic composition, we used a two-member mixing model as flood contribution = $(\delta D_{ped,\ post\text{-}flood} - \delta D_{ped,\ pre\text{-}flood}) / (\delta D_{floodwater} - \delta D_{ped,\ pre\text{-}flood})$. There is uncertainty in pre-flood moisture content and δD because we used control peds to estimate those values rather than measuring the treated peds themselves, and there was additional, analytical uncertainty in δD, so we could make only coarse estimates of flood contributions. In the case of

292 δD, apparent flood contributions potentially included mass flux of floodwater into peds as well
293 as diffusional mixing of floodwater with pre-flood water.

294 ### 2.5 Physical Properties of Peds

295 After measuring dye coverage and stable water isotopes, each ped (treatment and control) was
296 measured for gravimetric moisture content (mass loss upon drying at 105°C as a proportion of
297 oven-dry mass) and organic matter content (percent mass loss on ignition at 550°C). Because of
298 the high clay content, loss-on-ignition is an overestimate organic matter by likely 4-6% for our
299 soils (Ball 1964). We quantified the size of peds by mass and moisture content gravimetrically
300 because void ratio varies by moisture content in vertic clays and usurps the meaning of
301 properties based on soil volume. Particle size analysis was performed on a 20 g mixed sample
302 from each soil depth class Samples were prepared using mechanical and chemical deflocculation
303 using sodium hexametaphosphate and removal of organic matter using H_2O_2. Prepared samples
304 were then run through a laser diffraction particle size analyzer (S3500, Microtrac,
305 Montgomeryville, PA, USA) assuming irregular particle shapes, transparent absorption
306 coefficient, and a preset refractive index for clay (Özer et al., 2010; Jena et al., 2013). Soil
307 texture was approximately 2% sand, 60% silt, and 38% clay (Table B.1), using the USDA
308 texture size classes of clay ≤ 2.00 μm. The silt was very fine and most bordered on clay size: 15
309 percent of the particles were between 2 and 3 μm. Because particle size analysis using the laser
310 diffraction method overestimates the size of particles as compared to the traditional sieve-pipette
311 method (Beuselinck et al. 1998), it is likely that the clay fraction was underestimated. Organic
312 matter decreased with depth across all peds (Figure 3a).
313
314
315

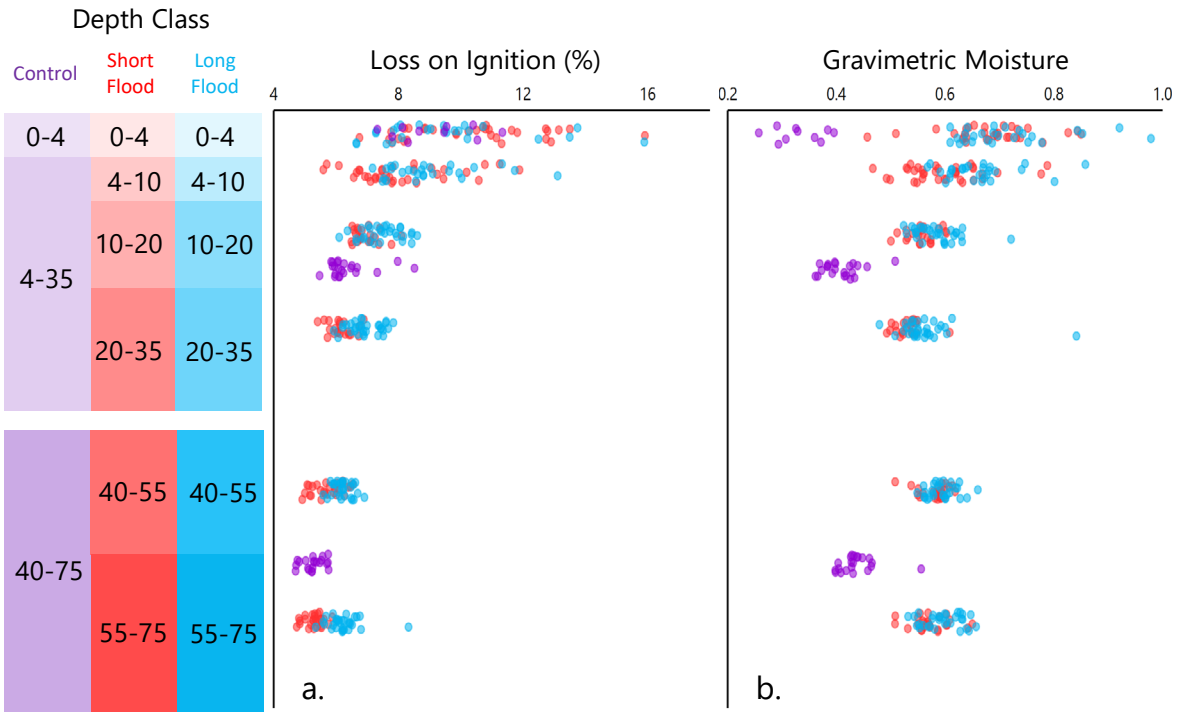

Figure 3. (**a**) Organic matter estimated by mass loss on ignition (likely 4-6% overestimated) and (**b**) gravimetric moisture of control and artificially flooded soil peds. Data were collected in depth classes and are presented with randomly jittered vertical positions for visibility. Differences in organic matter between short-flood and long-flood samples are coincidental.

3 Results

Flooding caused gravimetric moisture content to increase across all depths from 0.40 ± 0.05 g/g (mean ± SD) in the control peds to 0.59 ±0.07 g/g after the first 3–4 days, and then to 0.62 ± 0.08 from 3–4 to 31–32 days (Figure 3b). Thus, artificial flooding contributed much more (47% increase) at the onset of artificial flooding (i.e., the initial 3–4 days) than it did over the rest of the flood period (5% additional increase). Gravimetric moisture content in the control soil increased with depth but moisture content in the flooded peds decreased with depth after both flood durations. Gravimetric moisture content increased for all depth classes from short to long flood durations, although not statistically significantly at 0–4 cm (two-sample *t*-test; $p = 0.166$) or 40–55 cm ($p = 0.084$) depths. Due to experimental design, the surfaces of depth classes 0–4 cm and 40–55 cm both received greater exposure to treatment water and less confining pressure from the surrounding soil than the other depth classes, thus providing more room for those peds to expand and increase moisture. Gravimetric moisture in the control peds decreased with

organic matter content because the soil was drier at the surface, while water increased with organic matter content after both flood durations because the soil was wetter at the surface (Figure 3b).

In general, dye coverage on ped surfaces declined with depth for both flood durations (Figure 4). Dye penetration did not occur more than a few mm into the soil matrix. For both artificial flood durations, dye coverage on surface peds was greatest in the 0–4 cm depth class and least in the 40–55 cm depth class (Figure 4a and b). There was no distinct pattern in differences of dye coverage with depth between flood durations, but many depths showed no change or even relatively less dye coverage for the long flooding event compared to the short (Figure 4c). There was generally greater dye coverage near the lateral boundaries but those peds were omitted because of sampling disturbance.

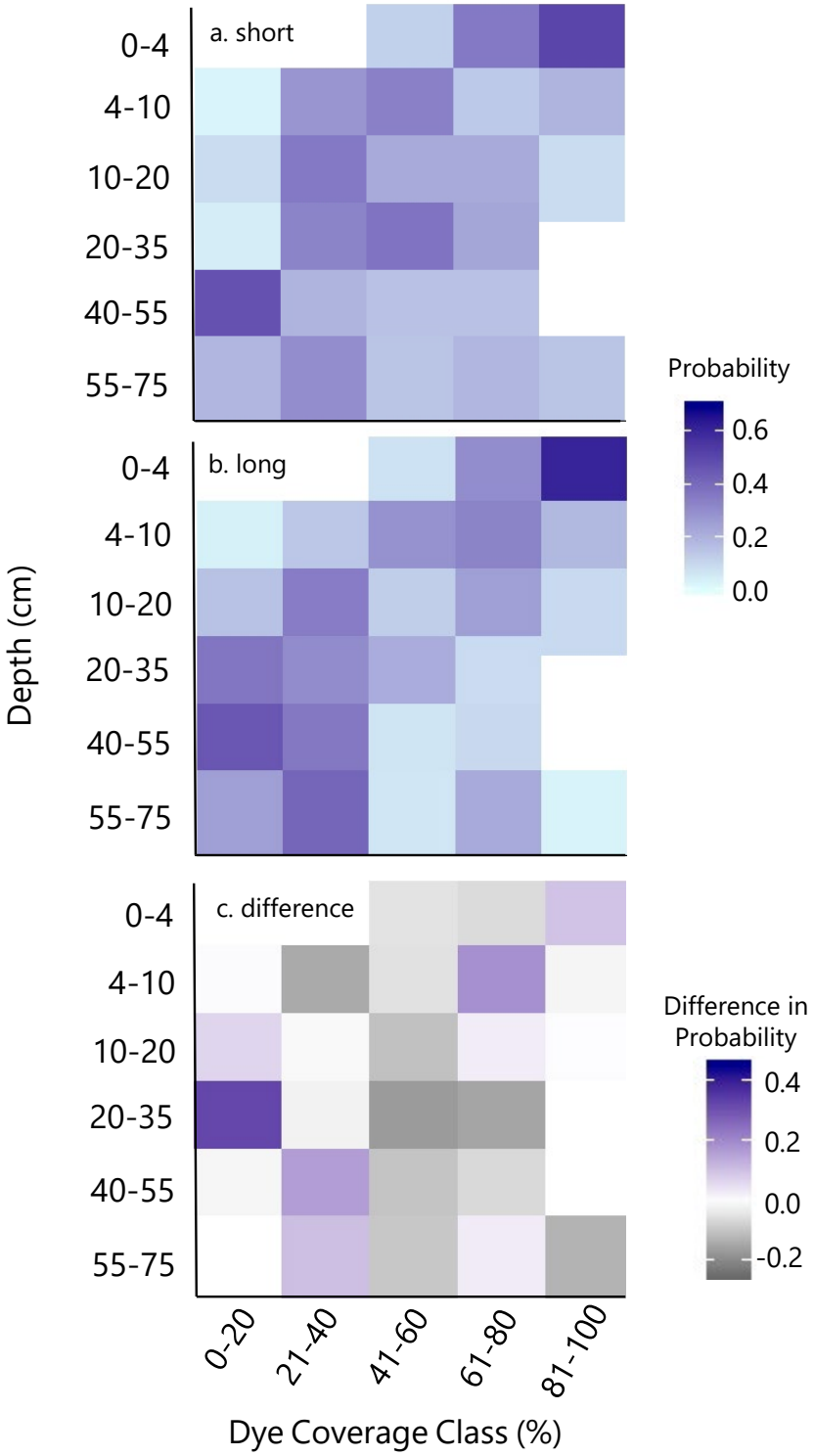

Figure 4. Probability of dye staining of ped surfaces by depth class in the (**a**) short and (**b**) long experimental floods and (**c**) the difference in frequency between the two durations of artificial flooding.

In some peds, particularly those near the surface, deuterium concentration indicated pre-event water was almost completely replaced by flood water, but even after 32 days there was incomplete replacement of pre-event water at depth (Figure 5). After the short-duration flood, apparent isotopic contribution of the artificial flood water ranged from ~60–115% within 10 cm of the surface and mostly ~20–40% at depth. After the long-duration flood, apparent isotopic contribution of the artificial flood water exceeded ~90% within 10 cm of the surface and ~60–80% at depth. Ped water was more enriched in δD for the long flood duration (mean +59‰, compared to artificial floodwater of +70‰) than the short flood duration (mean +41‰, compared to artificial floodwater of +68‰) across all depth classes, indicating increasing content of artificial flood water in the ped matrix over time. The short-duration flooding was also associated with greater ranges of ped δD, indicating spatial variability in the absorption of flood water and diffusional exchange of deuterium. The smallest difference in δD between durations was at depth class 0–4 cm, where flood water dominated matrix water for both durations. In general, the differences in flood-water dominance between durations increased with depth. Ped water δD decreased with depth in the control peds (from +3‰ at the surface to -15‰ at 65 cm depth), yet those variations were small relative to the effects of the tracer addition.

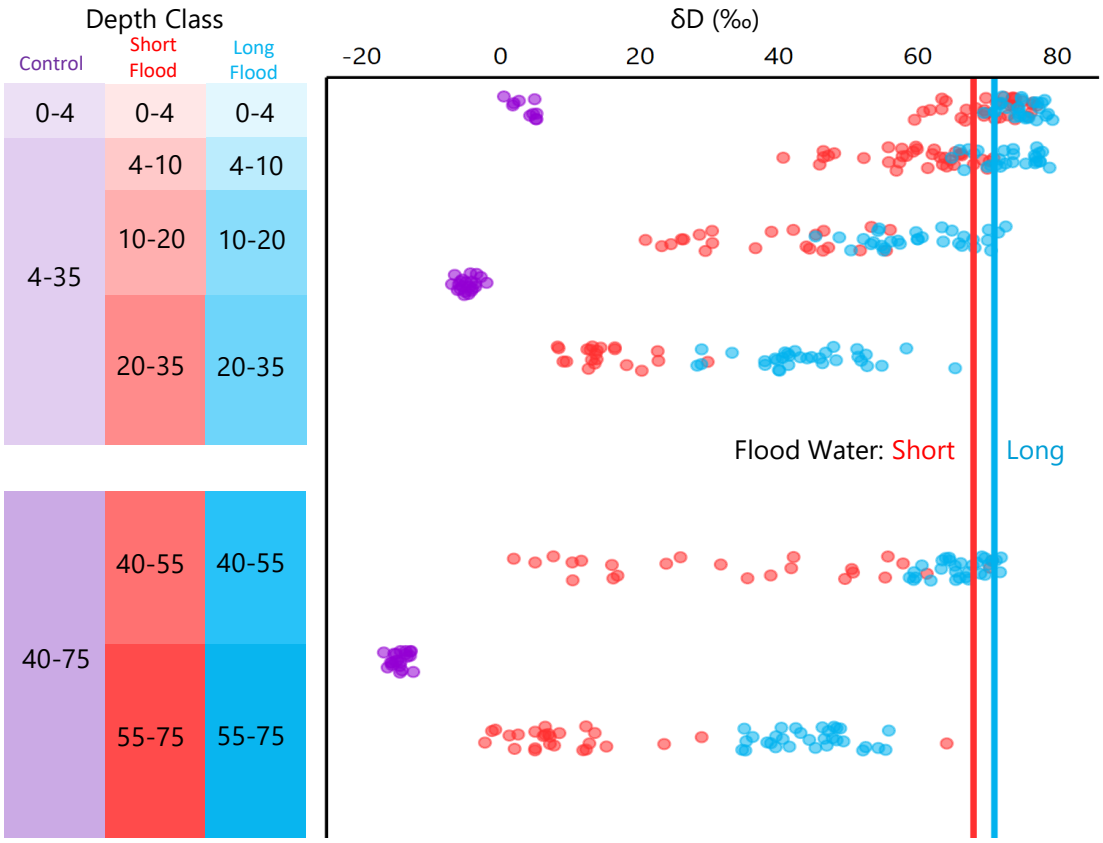

Figure 5. Concentration of deuterium in soil water from peds subjected to short- and long-duration artificial flooding by water spiked with deuterium to the indicated concentrations. Data were collected in depth classes and are presented with randomly jittered vertical positions for visibility.

Ped water δD was generally higher (i.e., more apparent flood water) than the expected δD given mean moisture content differences between flooded peds and control peds (Figure 6). Isotopic equilibration with the flood water was essentially complete (isotopic composition >90% of flood water) for 30% of peds in the short-duration flood and 51% of peds in the long-duration flood. Soil water δD in 25% of peds from the short-duration flood was within the bounds of expected δD given the mass change imparted by flooding and thus showed no evidence of equilibration by diffusion beyond mass influx. These samples were clustered at the low end of measured (and expected) δD values, indicating that these samples had limited wetting during the initial 3–4 days of flooding. In contrast, all peds from the long-duration flood contained more deuterium than expected given their increase in moisture content, indicating measurable equilibration with experimental flood water. Isotopic equilibration was greater at the tops of the monoliths—where expansion was least constrained—than it was at depth (Figure 5).

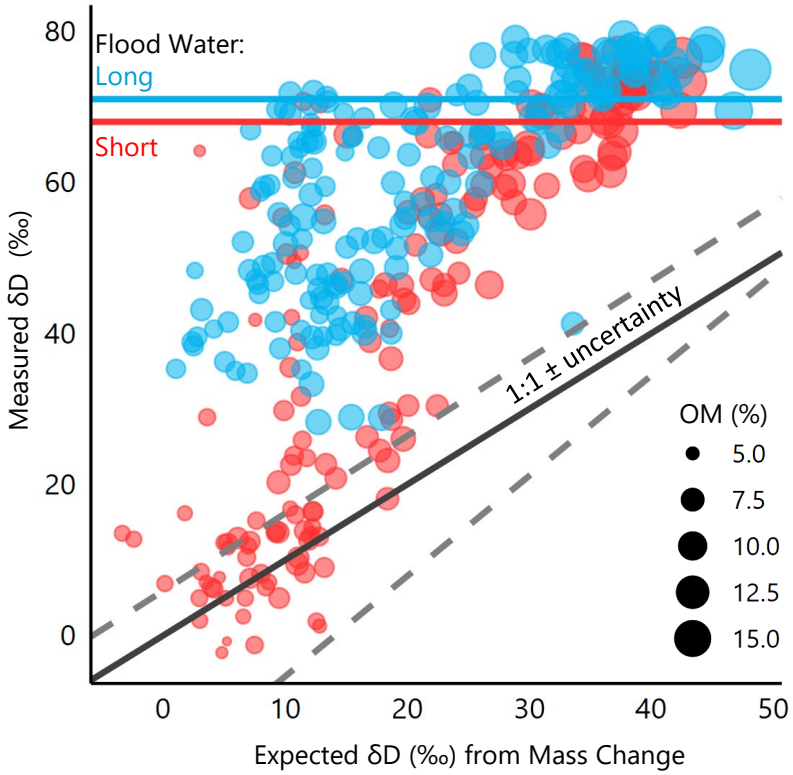

Figure 6. Deuterium concentrations in soil water compared to expected concentrations given deviation in sample peds from mean moisture content and δD of control peds by depth. Dashed lines indicate bounds of uncertainty, obtained by applying maximum or minimum observed δD and moisture content of control peds by depth.

Much of the variance in ped-water δD was related to organic matter (Figure 7), likely because peds containing more organic matter absorbed more flood water (Figure 3a). Ped-water δD increased with organic matter until the latter reached approximately 9% (Figure 7). Above 9% organic matter, almost all peds were dominated by flood water and there was little variation of δD. The degree of equilibration (i.e., δD greater than expected given mass influx alone) was not clearly related to organic matter content (Figure 6).

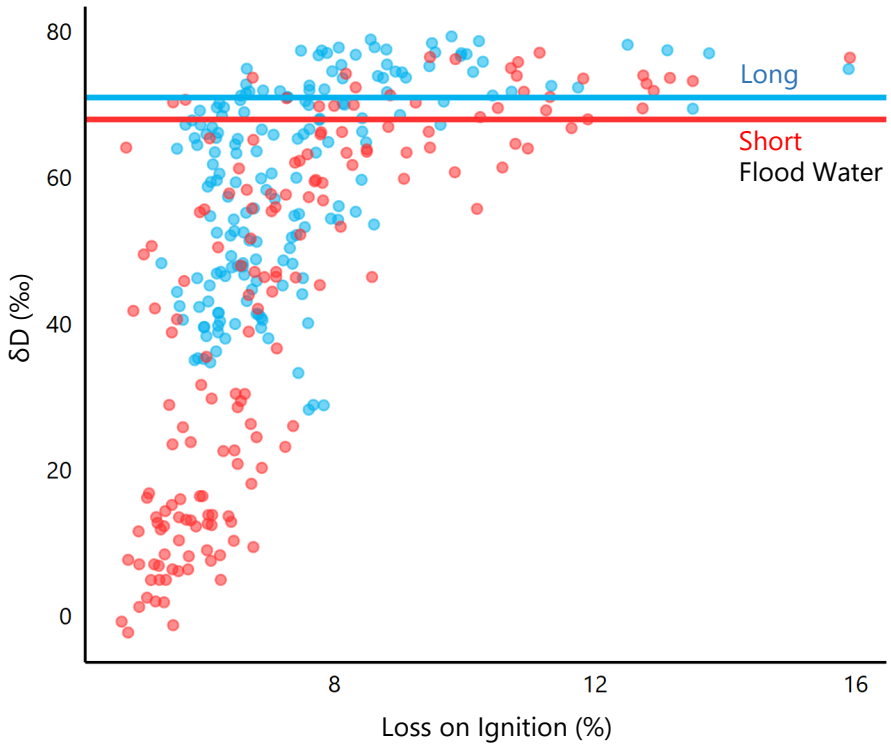

401

402 **Figure 7**. Concentration of deuterium in soil water from peds subjected to short- and long-duration
403 artificial flooding by water spiked with deuterium to the indicated concentrations, as a function of organic
404 matter estimated by mass loss on ignition (likely 4-6% overestimated).

405

406 Deuterium concentration increased with dye coverage for both flood durations, although
407 variability among peds was high (Figure 8). Dye coverage was a poor predictor of δD, except
408 that peds completely covered by dye tended to be dominated by flood-event water. In the short-
409 flood treatment, water in 41% of peds remained less than 50% derived from the flood event,
410 including 10% of peds that were nearly completely covered by dye. Although dye coverage did
411 not increase between the short and long flood durations (Figure 4), δD continued to shift toward
412 flood event water with the longer flood duration. After the long-duration flood, 92% of peds that
413 were at least 80% covered by dye also contained more than 80% flood water.

414

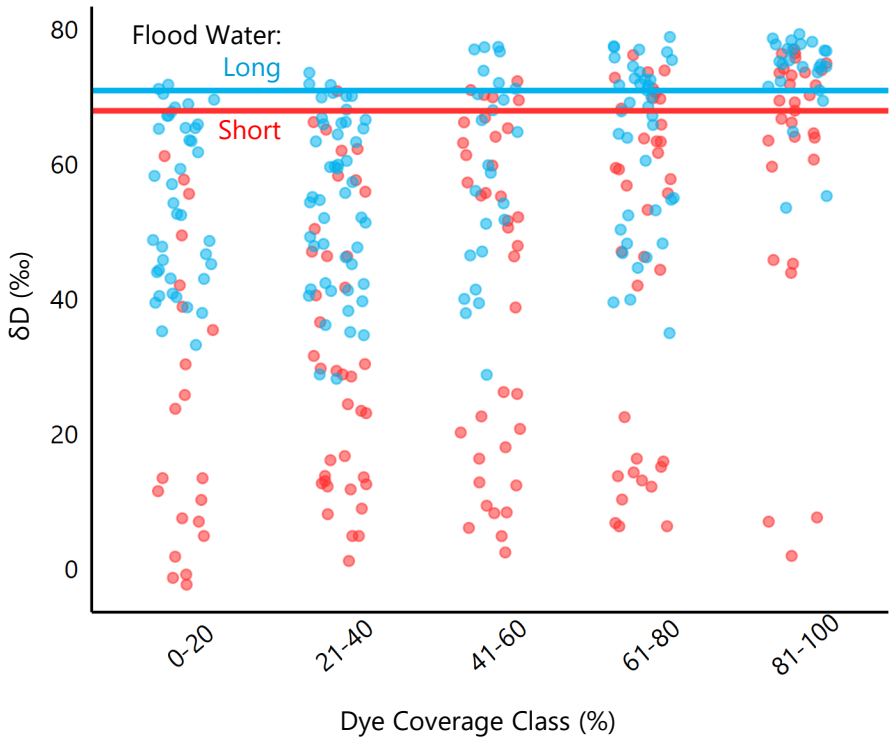

Figure 8. Concentration of deuterium in soil water from peds subjected to short- and long-duration artificial flooding by water spiked with deuterium to the indicated concentrations, as a function of dye coverage per ped. Data were collected in dye coverage classes and are presented with randomly jittered horizontal positions for visibility.

4 Discussion

The vertic properties of our experimental soil had a strong apparent effect on moisture recharge by flooding: soil moisture increased relatively little at depth as compared to the surface and remained relatively constant after initial wetting even under continued inundation. The small changes in water content at depth we observed are consistent with general soil moisture patterns observed in other vertic clays in response to both flooding and rainfall. For example, Miller & Bragg (2007) found relatively small differences in gravimetric moisture content at 100 cm between soil under extended ponding and soil in prolonged seasonally dry conditions. Slabaugh (2006) found relatively constant soil moisture with little apparent response to precipitation at depths of 25–200 cm for two Vertisols in Mississippi, USA, over a 6-month period. There, subsoil moisture content varied by only ± 4% annually, which is comparable to the 3% increase found between the short and long artificial flood durations found in this experiment. Pettry & Switzer (1996) reported consistent soil moisture despite precipitation variation in four Vertisols

433 in Mississippi, USA, over a 5-year period. They found the greatest moisture content and 80% of
434 the total variation in soil moisture in the upper 50 cm.
435
436 Results indicate matrix recharge is a two-step process, beginning with rapid mass flux via
437 macropores into peds during initial wet-up, followed by a period of isotopic equilibration
438 between soil matrix and flood waters. The relatively unchanging moisture content and similarity
439 of macropore connectivity (dye staining) between flood-duration treatments are consistent with
440 many investigations of infiltration of rainfall into vertic soils, in which mass water flux declines
441 rapidly because of crack closure (e.g., Favre et al., 1997). The subsequent increase in δD beyond
442 expected concentrations from mass changes in our peds indicates that diffusion continued to be
443 an important process after initial wet-up.
444
445 Many studies in floodplains and other low-lying agricultural soils have shown a longer-term
446 swelling response when Vertisols become flooded. For example, Miller & Bragg (2007) found
447 top-down, episaturation of field soil, with low moisture content variation at depth, similar to our
448 experiment, in both ponded and non-ponded forested Vertisols in Texas, USA. They reported
449 that, during ponded conditions, ped interiors were wet (≥50% gravimetric soil water content and
450 soil glistened) down to 30 cm during the first two weeks of ponding and down to 50 cm after 3
451 weeks. McIntyre et al. (1982) showed that swelling continued for several months as moisture
452 slowly moved downward through the profile. These studies point to episaturation, in which near-
453 surface layers become saturated before deeper ones, acting as a restriction on downward water
454 movement and recharge.
455
456 In our experimental design the monoliths were submerged into flood waters, meaning that water
457 could infiltrate from all directions. This approach reduced episaturation, and as a result the
458 wetting behaviors observed in our study (rapid saturation followed by little change in water
459 content) were more similar to those observed in studies conducted in well-structured upland clay
460 soils where macropores give access through more of the soil profile (e.g., Stewart et al., 2015;
461 Navar et al., 2002). At the same time, most of the change in soil water content in our experiment
462 occurred in the uppermost layers. This result has analogs in several field studies of Vertisols,
463 which showed that near-surface soils (e.g., the upper 50 cm) experience the majority of moisture

fluctuations under typical field conditions (Pettry & Switzer, 1996; Slabaugh, 2006; Miller & Bragg, 2007).

Taken altogether, our results and results from previous experiments suggest that flood duration may be an important factor in water recharge for soils that experience episaturation, because gradients apparently favor continued but slow downward flux. In contrast, flood duration appears to be less important in soils with persistent flow pathways (e.g., root channels), perhaps because gradients are weaker when they are not all vertical. For these soils, the frequency of flooding and drying cycles may instead represent a more important control on soil water recharge.

By inhibiting episaturation, our experimental design allowed us to isolate relative effects of clay swelling, confining pressures, and organic matter on water movement in Vertisols. Soil moisture in Vertisols is strongly influenced by confining pressures within the soil that resist swelling and thus limit moisture (Groenevelt & Bolt 1972). Because the monoliths were divided into two pieces (0–35 and 40–75 cm), confining pressure was removed from the upper portion of the lower section. As a result, overburden pressure was low in both the 0–10 cm (i.e., 0–4 and 4–10 cm) and 40–55 cm depth increments, yet these layers differed in organic matter (Figure 3a). The lack of confining pressure likely allowed greater increases in water content and δD in the 40–55 cm depth increment compared to the 20–35 cm depth (Figures 3b and 5). Likewise, there was much less variability in δD in the 40–55 cm depth class during the long artificial flood duration, suggesting that the greater swelling in that horizon facilitated greater isotopic exchange. However, the post-flooding water contents and mean δD of the 40–55 cm depth class were still lower than those at 0–10 cm, where there were many more fine roots, higher organic matter, and greater dye staining. Studies on bare soils have shown that surface crusting and sealing can force nearly all infiltrating water into cracks (e.g., Wells et al., 2003), but organic matter at the surface of our soil promoted uptake into peds. Thus, organic matter appears to be an important factor for mass flux and isotopic exchange in forested floodplain soils, regardless of flood duration.

Air entrapped in our experimental monoliths may have contributed to some phenomena we observed. Although rapid immersion in floodwater creates the possibility for rapid flow in soil cracks before swelling and crack closure, it may also inhibit water flux in those same pathways if

rapid immersion fills macropores and prevents air escape, thus decreasing the overall infiltration rate. Therefore, some peds that lacked dye staining in our experiment may have been adjacent to air bubbles instead of closed macropores. Entrapped air can also serve as a pathway for isotopic exchange, so that isotopic equilibration between ped water and floodwater may have included some vapor pathways.

Dye coverage on ped faces was a poor predictor of isotopic composition of ped water after the artificial floods. From this, we conclude that uptake into peds is also preferential, particularly deep in the soil profile where organic matter and porosity were lower and confining stresses resisting swelling were higher. Diffusion-driven water exchange caused the ped water to become more isotopically similar to the flood water through time. However, even after one month, deeper peds continued to be depleted in D relative to the source water. While the exchange process likely would continue through time and eventually render a homogenous isotopic signature throughout, these results suggest that soil water isotopes can resist mixing over short- to intermediate- timescales. The differences between the 20–35 cm depth class (median δD of +42‰; ~66% event water) and 40–55 cm depth class (median δD of +65‰; ~91% event water) suggest that soil swelling likely also influences isotopic exchange. The swelling process allowed the soil peds to uptake greater quantities of flood water (explaining the greater initial δD increase in the 40–55 cm depth) and may have created bigger shifts in pore size distribution, which could facilitate more rapid exchange. Indeed, previous work has posited that small pores may be the most effective at retaining distinct pools of water that do not equilibrate (e.g., Sprenger et al. 2019).

Our results are useful for interpreting whether there is distinct water pool partitioning between plant-available and runoff water—such as described by the “two water worlds” (TWW) hypothesis (Brooks et al., 2010)—in floodplain soils with shrink-swell properties. The interpretation of our results in terms of TWW depends on the mechanisms by which runoff occurs. If low permeability leads to dominance of episaturation, ponding, and surface runoff flowpaths, plant-available water is likely separate from runoff and dominated by the initial event water. However, ponding and surface runoff are not the dominant runoff mechanism at all sites with vertic soils because preferential flowpaths through soils can generate runoff from

526 subsurface flowpaths (Allen et al. 2005), potentially even at higher soil moisture when surface
527 cracks have closed (Baram et al. 2012). Also, even under saturated conditions, there may be
528 continued subsurface flux through other preferential pathways such as root channels that do not
529 seal from swelling (Ritchie et al. 1972). Our results suggest that residence times of more than
530 one month would be required for complete isotopic equilibration between runoff and plant-
531 available water for the deeper soils, but that equilibration in the uppermost ~10 cm of floodplain
532 Vertisols is likely to be rapid. Fine roots in this ecosystem are concentrated in the top ~20 cm of
533 soil (Farrish 1991) where moisture is most responsive to precipitation (Pettry and & Switzer,
534 1996; Slabaugh, 2006; Miller and & Bragg, 2007), so water lower in the profile where
535 equilibration is slower may not be important as direct plant water sources, and there may be little
536 separation between runoff and plant-available water. To the degree that plants access water
537 below the surface, organic-rich layer, there is likely to be strong separation between plant-
538 available and runoff water in Vertisols, but due to preferential flowpaths along root paths rather
539 than the commonly cited reason of the soil moisture release curve (Brooks et al., 2010; Evaristo
540 et al., 2015; Goldsmith et al., 2012).

541 **5 Conclusions**

542 Artificial flooding of soil monoliths revealed the processes by which inundation recharges soil
543 matrix water in the presence of connected macropore networks. Soil water content increased
544 rapidly in the initial three days of wetting, whereas over a subsequent four-week period
545 molecular diffusion was the dominant mode of water exchange. There was a high degree of dis-
546 connectivity between infiltrating flood and internal ped water, so there are some moisture stores
547 of long residence time and low exchange with the more-rapid fluxes in the macropore network.
548 Soil swelling and organic matter are both important factors controlling water flux into the soil
549 matrix, so that near-surface peds quickly become dominated by event water but some deeper,
550 confined peds with low organic matter may only exchange minor amounts of water. Macropores
551 are active and dominate during the initial flood, but macropore flux ceases relatively quickly,
552 resulting in diffusional processes recharging the matrix beyond initial wet-up. This poor
553 connectivity of macropores to the matrix explains field observations of steady soil moisture,
554 episaturation, and lack of connectivity between surface and subsurface water pools in vertic

555 soils. We conclude that flooding has a rapid and large impact on soil moisture, but that neither
556 the water nor chemistry of flood waters are comprehensively transmitted to the entire soil profile.

557 **Acknowledgments and Data**

558 United States Department of Agriculture (USDA) National Institute of Food and
559 Agriculture, project LAB94374, provided financial support for research studies contributing to
560 this manuscript. Funding for this work was provided in part by the Virginia Agricultural
561 Experiment Station and the Hatch Program of the National Institute of Food and Agriculture,
562 USDA (1007839). Any opinions, findings, conclusions, or recommendations expressed in this
563 publication do not necessarily reflect the view of the USDA. The authors declare no conflicts of
564 interest. Data can be obtained from the USDA Ag Data Commons at
565 https://data.nal.usda.gov/dataset/data-matrix-recharge-vertic-forest-soil-flooding-0. The dataset
566 DOI is 10.15482/USDA.ADC/1520928.

567 **References**

568 Allen, P. M., Harmel, R. D., Arnold, J., Plant, B., Yelderman, J., & King, K. (2005). Field data
569 and flow system response in clay (Vertisol) shale terrain, north central Texas, USA.
570 *Hydrological Processes*, *19*(14), 2719–2736. https://doi.org/10.1002/hyp.5782
571
572 Allen, S. T., Krauss, K. W., Cochran, J. W., King, S. L., & Keim, R. F. (2016). Wetland tree
573 transpiration modified by river-floodplain connectivity. *Journal of Geophysical Research*
574 *Biogeosciences*, *121*(3), 753–766. https://doi:10.1002/2015JG003208
575
576 Allen, S. T., Kirchner, J. W., Braun, S., Siegwolf, R. T., & Goldsmith, G. R. (2019). Seasonal
577 origins of soil water used by trees. *Hydrology and Earth System Sciences*, *23*(2), 1199–1210.
578 https://doi.org/10.5194/hess-23-1199-2019
579
580 Armstrong, A. C. (1983). The measurement of watertable levels in structured clay soils by means
581 of open augur holes. *Earth Surface Processes and Landforms*, *8*(2), 183–187.
582 https://doi.org/10.1002/esp.3290080210
583

584 Ball, D. F. (1964). Loss-on-ignition as an estimate of organic matter and organic carbon in non-
585 calcareous soils. *Journal of Soil Science*, *15*(1), 84–92. https://doi.org/10.1111/j.1365-
586 2389.1964.tb00247.x
587
588 Baram, S., Kurtzman, D., & Dahan, O. (2012). Water percolation though a clayey vadose zone.
589 *Journal of Hydrology*, *424–425*, 165–171. https://doi.org/ 10.1016/j.jhydrol.2011.12.040
590
591 Berghuijs, W. R., & Allen, S. T. (2019). Waters flowing out of systems are younger than the
592 waters stored in those same systems. *Hydrological Processes*, *33*(25), 3251–3254.
593 https://doi.org/10.1002/hyp.13569
594
595 Beuselinck, L., Govers, G., Poesen, J., Degraer, G., & Froyen, L. (1998). Grain-size analysis by
596 laser diffractometry: comparison with the sieve-pipette method. *Catena*, 32(3–4), 193–208.
597 https://doi.org/10.1016/S0341-8162(98)00051-4
598
599 Booltink, H.W.G., & Bouma, J. (1991). Physical morphological characterization of bypass flow
600 in a well-structured clay soil. *Soil Science Society of America Journal*, *55*(5), 1249–1254.
601 https://doi.org/10.2136/sssaj1991.03615995005500050009x
602
603 Bowling, D. R., Schulze, E. S., & Hall, S. J. (2017). Revisiting streamside trees that do not use
604 stream water: Can the two water worlds hypothesis and snowpack isotopic effects explain a
605 missing water source? *Ecohydrology*, *10*(1), e1771. https://doi.org/10.1002/eco.1771
606
607 Bouma, J., Jongerius, A., Boersma, O., Jager, A., Schoonderbeek. D. (1977). The function of
608 different types of macropores during saturated flow through four swelling soil horizons. *Soil*
609 *Science Society of America Journal*, *41*(5), 945–950.
610 https://doi.org/10.2136/sssaj1977.03615995004100050028x
611
612 Bouma, J., Dekker, L. W., & Haans, J. C. F. M. (1980). Measurement of depth to water table in a
613 heavy clay soil. *Soil Science*, *130*(5), 264–270.
614

615 Bouma, J., & Wösten, J. H. M. (1984). Characterizing ponded infiltration in a dry cracked clay
616 soil. *Journal of Hydrology*, *69*(1–4), 297–304. https://doi.org/10.1016/0022-1694(84)90169-0
617
618 Broadfoot, W. M. (1962). The fame of Sharkey clay. *Forests and People*, *12*(1), 30–31.
619
620 Bronswijk, J. J. B., Hamminga, W., & Oostindie, K. (1995). Field-scale solute transport in a
621 heavy clay soil. *Water Resources Research*, 31(3), 517–526. https://doi.org/10.1029/94WR02534
622
623 Brooks, J. R., Barnard, H. R., Coulombe, R., & McDonnell, J. J. (2010). Ecohydrological
624 separation of water between trees and streams in a Mediterranean climate. *Nature Geoscience*,
625 3(2), 100–104. https://doi.org/10.1038/ngeo722
626
627 Das Gupta, S., Mohanty, B. P., & Köhne, J. M. (2006). Soil hydraulic conductivities and their
628 spatial and temporal variations in a Vertisol. *Soil Science Society of America Journal*, *70*(6),
629 1872–1881. https://doi.org/10.2136/sssaj2006.0201
630
631 Farrish, K. W. (1991). Spatial and temporal fine-root distribution in three Louisiana forest soils.
632 *Soil Science Society of America Journal*, *55*(6), 1752–1757.
633 https://doi.org/10.2136/sssaj1991.03615995005500060041x
634
635 Favre, F., Boivin, P., & Wopereis, M. C. S. (1997). Water movement and soil swelling in a dry,
636 cracked Vertisol. *Geoderma*, *78*(1–2), 113–123. https://doi.org/10.1016/S0016-7061(97)00030-
637 X
638
639 Flury, M., Flühler, H., Jury, W. A., & Leuenberger, L. (1994). Susceptibility of soils to
640 preferential flow of water: A field study. *Water Resources Research*, *30*(7), 1945–1954.
641 https://doi.org/10.1029/94WR00871
642
643 Flury, M. & Fluhler, H. (1995). Tracer characteristics of Brilliant Blue FCF. *Soil Science Society*
644 *of America Journal*, *59*(1), 22–27. https://doi.org/10.2136/sssaj1995.03615995005900010003x
645

Gaj, M., A. Lamparter, S.K. Woche, J. Bachmann, J.J. McDonnell, & C.F. Stange. (2019). The role of matric potential, solid interfacial chemistry, and wettability on isotopic equilibrium fractionation. *Vadose Zone Journal*, *18*(1), 180083. https://doi.org/10.2136/vzj2018.04.0083

Good, S. P., Noone, D., & Bowen, G. (2015). Hydrologic connectivity constrains partitioning of global terrestrial water fluxes. *Science*, *349*(6244), 175–177. https://doi.org/10.1126/science.aaa5931

Goldsmith, G. R., Muñoz-Villers, L. E., Holwerda, F., McDonnell, J. J., Asbjornsen, H., & Dawson, T. E. (2012). Stable isotopes reveal linkages among ecohydrological processes in a seasonally dry tropical montane cloud forest. *Ecohydrology*, *5*(6), 779–790. https://doi.org/10.1002/eco.268

Greve, A., Anderson, M. S., & Acworth, R. I. (2010). Investigations of soil cracking and preferential flow in a weighing lysimeter filled with cracking clay soil. *Journal of Hydrology*, *393*, 105–113. https://doi.org/10.1016/j.jhydrol.2010.03.007

Groenevelt, P. H., & Bolt, G. H. (1972). Water retention in soil. *Soil Science*, *113*(4), 238-245.

Hardie, M., Doyle, R., Cotching, W., Holz, G., & Lisson, S. (2013). Hydropedology and preferential flow in the Tasmanian texture-contrast soils. *Vadose Zone Journal*, *12*(4) https://doi.org/10.2136/vzj2013.03.0051

Hoogmoed, W.B., & Bouma, J., (1980). A simulation model for predicting infiltration into cracked clay Soil. *Soil Science Society of America Journal*, *44*(3), pp.458–461. https://doi.org/10.2136/sssaj1980.03615995004400030003x

Jasechko, S., Sharp, Z. D., Gibson, J. J., Birks, S. J., Yi, Y., & Fawcett, P. J. (2013). Terrestrial water fluxes dominated by transpiration. *Nature*, *496*(7445), 347–350. https://doi.org/10.1038/nature11983

Jena, R. K., Jagadeeswaran, R., & Sivasamy, R. (2013). Analogy of soil parameters in particle size analysis through laser diffraction techniques. *Indian Journal of Hill Farming*, *26*(2), 78–83.

Ketelsen, H. & Meyer-Windel, S. (1999). Adsorption of brilliant blue FCF by soils. *Geoderma*, *90*(1–2), 131–145. https://doi.org/10.1016/S0016-7061(98)00119-0

Kishné, A. Sz., Morgan, C. L. S., Ge, Y., & Miller, W.L. (2010). Antecedent soil moisture affecting surface cracking of a Vertisol in field conditions. *Geoderma*, *157*(3–4), 109–117. https://doi.org/10.1016/j.geoderma.2010.03.020

Lamontagne, S., Leaney, F. W., & Herczeg, A. L. (2005). Groundwater–surface water interactions in a large semi-arid floodplain: implications for salinity management. *Hydrological Processes*, *19*(16), 3063–3080. https://doi.org/10.1002/hyp.5832

Lin, Y., & Horita, J. (2016). An experimental study on isotope fractionation in a mesoporous silica-water system with implications for vadose-zone hydrology. *Geochimica et Cosmochimica Acta*, *184*, 257–271. https://doi.org/10.1016/j.gca.2016.04.029

Lin, Y., Horita, J., & Abe, O. (2018). Adsorption isotope effects of water on mesoporous silica and alumina with implications for the land-vegetation-atmosphere system. *Geochimaca et Cosmochimica Acta*, *223*, 520–536. https://doi.org/10.1016/j.gca.2017.12.021

Majoube, M. (1971). Fractionnement en ^{18}O entre la glace et la vapeur d'eau. *Journal de Chimie Physique et de Physico-Chimie Biologique*, *68*, 1423–1436. https://doi.org/10.1051/jcp/1971680625

McIntyre, D., Watson, C., & Loveday, J. (1982). Swelling of a clay soil profile under ponding. *Soil Research*, *20*(2), 71–79. https://doi.org/10.1071/SR9820071

Miller, W. L., & Bragg, A. L. (2007). *Soil Characterization and Hydrological Monitoring Project, Brazoria County, Texas, Bottomland Hardwood Vertisols*. US Department of Agriculture, Natural Resources Conservation Service, Temple, TX (13 pp.).

Oerter, E., Finstad, K., Schaefer, J., Goldsmith, G. R., Dawson, T., & Amundson, R. (2014). Oxygen isotope fractionation effects in soil water via interaction with cations (Mg, Ca, K, Na) adsorbed to phyllosilicate clay minerals. *Journal of Hydrology*, *515*, 1–9. https://doi.org/10.1016/j.jhydrol.2014.04.029

Öhrström, P., Hamed, Y., Persson, M., & Berndtsson, R. (2004). Characterizing unsaturated solute transport by simultaneous use of dye and bromine. Journal of Hydrology, 289(1–4), 23–35. https://doi.org/10.1016/j.jhydrol.2003.10.014

Oshun, J., Dietrich, W. E., Dawson, T. E., & Fung, I., (2016). Dynamic, structured heterogeneity of water isotopes inside hillslopes. *Water Resources Research*, *52*(1), 164–189. https://doi.org/10.1002/2015WR017485

Özer, M., Orhan, M., & Işik, N. S. (2010). Effect of particle optical properties on size distribution of soils obtained by laser diffraction. *Environmental & Engineering Geoscience*, *16*(2), 163–173. https://doi.org/10.2113/gseegeosci.16.2.163

Pettry, D. E., & Switzer, R. E. (1996). *Sharkey Soils in Mississippi*. Mississippi Agriculture and Forestry Experiment Station Bulletin 1057 (37 pp.).

Ritchie, J. T., Kissel, D. E., & Burnett, E. (1972). Water movement in undisturbed swelling clay soil. *Soil Science Society of America Journal*, 36(6), 874–879. https://doi.org/10.2136/sssaj1972.03615995003600060015x

Römkens, M. J. M., & Prasad, S. N. (2006). Rain infiltration into swelling/shrinking/cracking soils. *Agricultural Water Management*, *86*(1-2), 196–205. https://doi.org/10.1016/j.agwat.2006.07.012

Slabaugh, J. D. (2006). *Final Report: Of Data from the Study of Sharkey Soils in the Lower Mississippi Valley*. US Department of Agriculture, Natural Resources Conservation Service, Little Rock, AR (65 pp.).

Sprenger, M., Llorens, P., Cayuela, C., Gallart, F., & Latron, J. (2019). Mechanisms of consistently disjunct soil water pools over (pore) space and time. *Hydrology and Earth System Sciences*, *23*(6), 2751–2762. https://doi.org/10.5194/hess-23-2751-2019

Stewart, R. D., Abou Najm, M. R., Rupp, D. E., Lane, J. W., Uribe, H. C., Arumí, J. L., & Selker, J. S. (2015). Hillslope run-off thresholds with shrink–swell clay soils. *Hydrological Processes*, *29*(4), 557–571. https://doi.org/10.1002/hyp.10165

Stewart, R. D., Abou Najm, M. R., Rupp, D. E., & Selker, J. S. (2016a). A unified model for soil shrinkage, subsidence, and cracking. *Vadose Zone Journal*, *15*(3). https://doi.org/10.2136/vzj2015.11.0146

Stewart, R. D., Abou Najm, M. R., Rupp, D. E., & Selker, J. S. (2016b). Modeling multi-domain hydraulic properties of shrink-swell soils. *Water Resources Research*, *52*(10), 7911–7930. https://doi.org/10.1002/2016WR019336

Vargas, A. I., Schaffer, B., Yuhong, L., & Sternberg, L. D. S. L. (2017). Testing plant use of mobile vs immobile soil water sources using stable isotope experiments. *New Phytologist*, *215*(2), 582–594. https://doi.org/10.1111/nph.14616

Wassenaar, L. I., Hendry, M. J., Chostner, V. L., & Lis, G. P. (2008). High resolution pore water δ^2H and $\delta^{18}O$ measurements by $H_2O_{(liquid)}$-$H_2O_{(vapor)}$ equilibration laser spectroscopy. *Environmental Science and Technology*, *42*(24), 9262–9267. https://doi.org/10.1021/es802065s

Weiler, M. & Flühler, H. (2004). Inferring flow types from dye patterns in macroporous soils. *Geoderma*, *120*(1), 137–153. https://doi.org/10.1016/j.geoderma.2003.08.014

Wells, R. R., DiCarlo, D. A., Steenhuis, T. S., Parlange, J. Y., Römkens, M. J. M., & Prasad, S. N. (2003). Infiltration and surface geometry features of a swelling soil following successive simulated rainstorms. *Soil Science Society of America Journal*, *67*(5), 1344–1351. https://doi.org/10.2136/sssaj2003.1344

Yasuda, H., Berndtsson, R., Persson, H., Bahri, A., & Takuma, K. (2001). Characterizing preferential transport during flood irrigation of a heavy clay soil using the dye Vitasyn Blau. *Geoderma*, *100*(1–2), 49–66. https://doi.org/10.1016/S0016-7061(00)00080-X